JOURNAL OF AIRCRAFT
Vol. 31, No. 2, March–April 1994

Alleviation of Side Force on Tangent-Ogive Forebodies Using Passive Porosity

Steven X. S. Bauer*
NASA Langley Research Center, Hampton, Virginia 23665
and
Michael J. Hemsch†
Lockheed Engineering and Sciences Company, Hampton, Virginia 23666

An experimental investigation to determine the effectiveness of passive porosity for alleviating side forces on forebodies was conducted in the NASA Langley Research Center 7-ft by 10-ft high-speed wind tunnel. Force, moment, and surface pressure data were obtained on solid and porous (22% porosity, 0.020-in. hole diam) tangent-ogive forebodies of fineness ratios 2.5 and 5.0. The solid forebodies were tested with transition grit to simulate fully turbulent conditions, and without transition grit to simulate free transition conditions. The extent of porosity on the forebodies was varied to determine the extent of porosity needed to alleviate side forces. Static longitudinal and lateral-directional stability and surface pressure data were obtained at Mach numbers of 0.2, 0.5, and 0.8, angles of attack from −5 to 45 deg, and roll angles from −90 to 180 deg. The solid forebodies exhibited large asymmetric pressure loads at moderate to high angles of attack causing large side forces and yawing moments; the transition grit had minimal effect on the asymmetric characteristics, but had a large effect on the longitudinal characteristics. The porous forebodies exhibited no significant side forces or yawing moments at any angle of attack tested.

Nomenclature

C_N = normal force coefficient
C_p = pressure coefficient
C_Y = side force coefficient
D = model base diameter, 4 in.
h = height at model base in the z direction, 2 in.
M_∞ = freestream Mach number
S_{ref} = reference (base) area
x = axial distance, in streamwise direction
y = model reference direction as defined in Fig. 10
z = model reference direction as defined in Fig. 10
α = angle of attack, deg
ΔC_p = $(C_p)_{\text{right-hand side}}-(C_p)_{\text{left-hand side}}$
φ = roll angle measured from bottom of model as defined in Figs. 6, 7, 9, and 10

Introduction

AT high angles of attack, axisymmetric bodies can exhibit a side force, even at zero sideslip angle. This side force is a result of asymmetric pressure loading caused by differences in the location of the separation induced vortex on either side of the forebody. This phenomena has been documented extensively.[1–3] Numerous studies have been conducted to develop devices which eliminate or minimize the asymmetric behavior of forebodies.[4–8] These "fixes" typically involve reshaping the nose or adding devices, such as strakes, to the existing geometry which add weight and are beneficial for only a limited range of conditions. In the present study, a passive porous system is investigated to alleviate the asymmetric loading on the forebody. In the studies done by Keener et al.,[9–12] it was found that a tangent-ogive forebody with fineness ratio of 3.5 produced large asymmetries beginning at an angle of attack between 30 and 35 deg at a Mach number of 0.25. From these results, tangent-ogive forebody models of fineness ratios 2.5 and 5.0 were fabricated. These forebodies were predicted to encounter asymmetric loading conditions at angles of attack above (2.5-caliber forebodies) and below (5.0-caliber forebodies) that found for the 3.5-caliber forebodies documented by Keener.

Previous tests of passive porous cavities on airfoils in transonic flowfields[13–18] showed that the shock strength could be reduced, which also reduced the amount of shock-induced separated flow. Various other applications of porosity have been studied[19–23]; in each study the concept used the higher pressure behind a shock to provide a high plenum pressure which would feed the boundary layer upstream of the shock. It was found that the pressure within the plenum equalized even where large gradients existed above the porous surface. Because of this equalization of pressure, it was postulated that porosity could be applied to forebodies to eliminate any asymmetric forces. A porous outer skin was attached to a solid supporting centerbody. A plenum was created between the two surfaces. The plenum is likely to affect asymmetric side force generation in two ways: 1) by reducing the circumferential surface pressure gradients and 2) by equalizing the surface pressures left-to-right. The former effect would reduce the generation of vorticity in the boundary layer, thus minimizing the strength of the vortex system. The latter effect would help keep the vorticity generation symmetric.

Three Mach numbers (0.2, 0.5, and 0.8) were chosen to provide a wide speed range to determine the effect of Mach number on the size of the side forces and yawing moments encountered. The 2.5-caliber forebodies were found to behave in a manner similar to the 5.0-caliber forebodies; however, the angle of attack where asymmetries occurred was higher and the asymmetries were weaker than for the 5.0-caliber forebodies. Therefore, only the data for the 5.0-caliber forebodies will be presented in this article.

Presented as Paper 92-2711 at the AIAA 10th Applied Aerodynamics Conference, Palo Alto, CA, June 22–24, 1992; received July 31, 1992; revision received Jan. 15, 1993; accepted for publication Feb. 5, 1993. Copyright © 1992 by the American Institute of Aeronautics and Astronautics, Inc. No copyright is asserted in the United States under Title 17, U.S. Code. The U.S. Government has a royalty-free license to exercise all rights under the copyright claimed herein for Governmental purposes. All other rights are reserved by the copyright owner.

*Aerospace Engineer, Supersonic/Hypersonic Aerodynamics Branch, Applied Aerodynamics Division. Member AIAA.
†Staff Engineer. Associate Fellow AIAA.

Modi et al.[24] discuss using porosity as well as delta strakes, nose-boom tips and their combination in eliminating undesirable side force on a conical pointed forebody. In the study presented here, the capability of the passive porous system for reducing the asymmetric loading at all pitch conditions was determined and a preliminary assessment of the extent of porous surface required to eliminate the asymmetries was also found.

Test Facility

The wind-tunnel tests were conducted in the NASA Langley Research Center 7-ft by 10-ft high-speed wind tunnel (HST). This tunnel is a closed-circuit, single-return, continuous-flow, atmospheric tunnel with a solid-wall test section 6.6 ft high, 9.6 ft wide, and 10 ft long. The tunnel is fan driven and is powered by a 14,000-hp electric motor. It operates over a Mach number range from approximately 0.0–0.9 to produce a maximum Reynolds number of 4×10^6/ft.[25]

Model Description

Four 30-in.-long wind-tunnel models were designed to show the effect of fineness ratio on the asymmetric loading of tangent-ogive forebodies and the effectiveness of passive porosity in alleviating these asymmetries. These four forebodies consisted of two solid and two porous models of fineness ratios 2.5 and 5.0. Shown in Fig. 1 is a photograph of the fineness ratio 5.0, porous forebody in the 7-ft by 10-ft high-speed wind tunnel. The hole size and porosity used on these models were established from a supersonic test conducted on a conical wing at supersonic speeds.[26] This test was an extension of transonic testing done by Nagamatsu.[13] In the test on the conical wing done by the first author, a porous cavity was situated parallel with the leading edge of the wing. It was determined that the crossflow shock strength could be reduced and the shock-induced separation could be eliminated, thus providing a reduction in drag. A porosity of 22% was found to give the largest reduction in shock strength (and thus, shock-induced separation), and a hole size of 0.020 in. in diameter or less was needed in order to prevent the formation of small shocks on the downstream side of the hole.

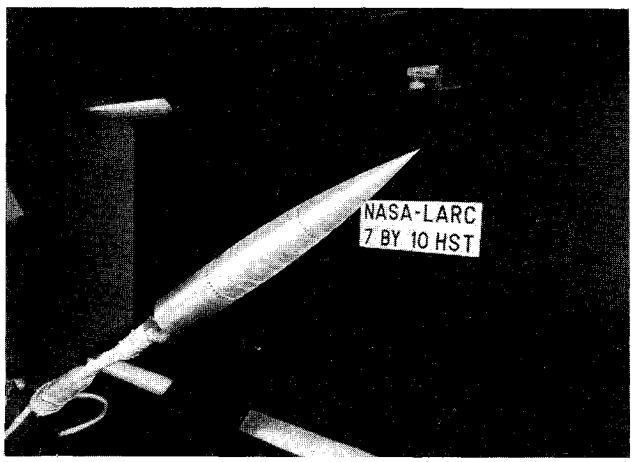

Fig. 1 Porous forebody model in 7-ft by 10-ft high-speed tunnel.

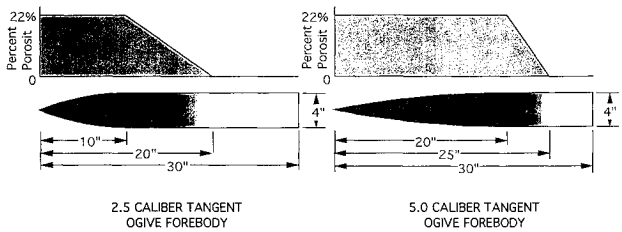

Fig. 2 Porous forebody model geometry and porosity distribution.

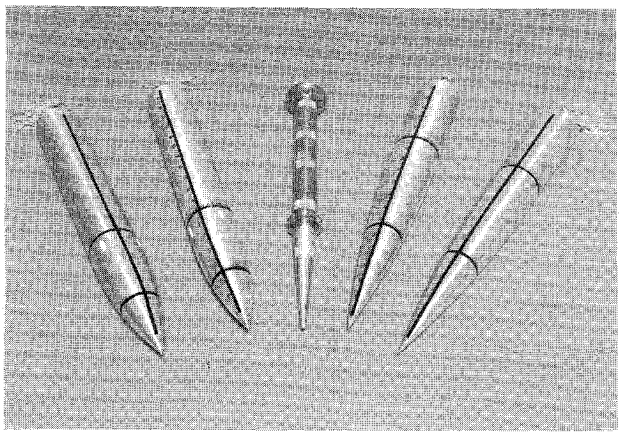

Fig. 3 Porous and solid forebody models and supporting centerbody.

The model geometries and porosity distributions are depicted in Fig. 2. The 2.5-caliber porous model had 22% porosity for the first 10 in. (i.e., the tangent-ogive forebody region), varied linearly from 22% to 0 porosity (i.e., solid surface) over the next 10 in., and was solid for the last 10 in. The 5.0-caliber porous model had 22% porosity over the first 20 in., varied linearly from 22% to 0 porosity over the next 5 in., and was solid for the last 5 in. A solid supporting centerbody was used to mount the four models on the sting and balance. The gap between the centerbody and outer shell forms a closed plenum region. Pressure probes were placed inside the plenum to determine if the plenum pressures were equalized and if any flow existed in the plenum.

A photograph of all of the models and the supporting centerbody is given in Fig. 3. The fineness ratio 2.5 tangent-ogive models are shown on the left, and the fineness ratio 5.0 tangent-ogive models are shown on the right with the porous bodies situated next to the supporting centerbody. Each of the models was equipped with 112 surface pressure orifices located at 1.25 and 3.00 calibers from the apex of the fineness ratio 2.5 models, and at 2.50 and 5.25 calibers from the apex of the fineness ratio 5.0 models. The pressure tubes from these orifices were routed between the model and the centerbody (in the plenum), out of four holes at the base of the centerbody, and along the sting to three 48-port electronic pressure gauges located on the model support mechanism within the test section.

Test Conditions and Procedures

The wind-tunnel test was conducted in the NASA Langley Research Center 7-ft by 10-ft HST. The tests were conducted under the conditions shown in Table 1.

Because pressure taps and holes can cause transition to turbulent flow,[27] it was expected that the porous models would have turbulent flow over most of the surface. To simulate this turbulent flow condition on solid bodies, number 80 sand grit was applied over the entire surface of each of the solid models. The grit size was chosen and applied to the model as explained by Hall et al.[28]

Force and moment and pressure data were obtained at angles of attack from −5 to 45 deg and zero sideslip. The

Table 1 Tunnel test conditions

Mach number	Reynolds number (per foot)	Reynolds number[a]
0.2	1.3 million	0.433 million
0.5	2.9 million	0.967 million
0.8	3.6 million	1.20 million

[a]Reynolds number based on base diameter of 4 in.

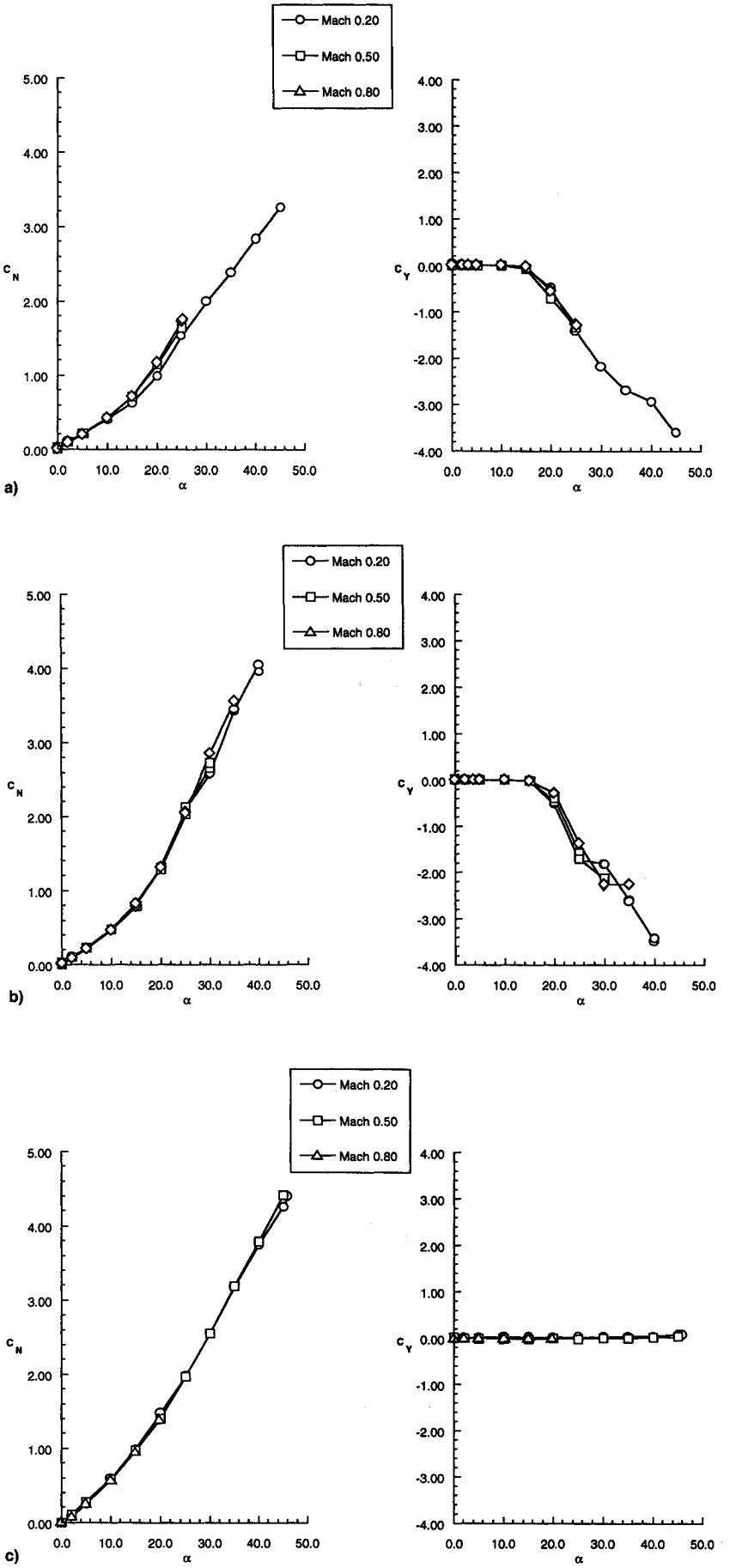

Fig. 4 Effect of Mach number on the normal-force and side-force characteristics of the 5.0-caliber forebodies, $\varphi = 0$ deg: a) solid body without transition grit, b) solid body with transition grit, and c) porous forebody.

models were also rolled to determine the conditions where asymmetric loadings due to small geometrical asymmetries occur. All angles of attack were corrected for sting and balance deflections. The force and moment data were measured by means of a six-component strain-gauge balance within the centerbody and connected to a supporting sting attached to the model actuating system in the tunnel.

Plenum pressures were measured using four pressure tubes attached to the solid centerbody. Base pressures were determined by two base pressure rings attached to the base of the centerbody. The pressures inside the balance housing (i.e., internal to the centerbody) were measured using two pressure tubes located on either side of the sting. All of these pressure tubes were routed along the sting to an electronic pressure transducer located several feet aft of the model within the test section. Force and moment data were corrected to free-stream static pressure at the model base and balance chamber.

Forebody Force and Moment Characteristics

Presented in Fig. 4 is the effect of Mach number on the normal-force and side-force characteristics of the fineness ratio 5.0 (i.e., 5.0 caliber) tangent-ogive forebodies. The C_N data for the solid body without transition grit (Fig. 4a) show a slight increase in C_N with increasing Mach number at angles of attack above 10 deg. The effect of Mach number on C_N for the solid forebody with transition grit (Fig. 4b) is much less (i.e., only at angles of attack above 30 deg). The porous forebody data (Fig. 4c) show no effect in C_N due to Mach number up to $\alpha = 40$ deg and only a slight variation at $\alpha = 45$ deg. The C_Y data for the three forebodies (i.e., solid without transition grit, solid with transition grit, and fully porous) do not exhibit a Mach number dependence, and the C_Y remains relatively low even at angles of attack up to 45 deg for the porous forebody. Because the normal force coefficients are nearly the same across the Mach number range, and because data at $M_\infty = 0.2$ could be obtained at higher angles of attack due to dynamics and loads exceeding balance limits for high angles of attack at Mach 0.5 and 0.8, the remainder of this article will focus on data for a Mach number of 0.2.

The effect of boundary-layer type (i.e., the application of transition grit) on the force characteristics is illustrated in Fig. 5. Three conditions are shown: 1) the porous forebody, 2) the solid forebody with no transition grit, and 3) the solid forebody with transition grit (i.e., fully gritted surface). The normal force coefficient values imply that the flow over the porous forebody behaves more like the fully turbulent condition than the free transition condition which has a much lower C_N value. The onset of asymmetric flow conditions have been found to correlate with the nose tip included angle.[29] For the fineness ratio 5.0 tangent-ogive forebody, the estimated onset angle is 23 deg. The side force coefficient data show that both the solid model without transition grit and the solid model with transition grit produce large side forces with the onset of the asymmetric loading conditions occurring at an angle of attack between 15–20 deg; the porous forebody has low C_Y values across the entire angle-of-attack range.

The models were rolled from −90 to 180 deg, and the values of C_N and C_Y plotted against φ to determine where asymmetric loading conditions due to small imperfections in the geometry occur.[30] Figure 6 presents the force characteristic data for the fineness ratio 5.0 tangent-ogive forebody at a Mach number of 0.2. Figure 6a illustrates data for the solid 5.0-caliber forebody without transition grit. Rolling the model had a great effect on both normal-force and side-force coefficient values due to geometrical asymmetries. The normal-force coefficient values for the solid 5.0-caliber forebody with transition grit (Fig. 6b) are nearly the same for all roll angles across the angle of attack range. Once again the side-force coefficient values show large asymmetric loadings due to geometrical asymmetries. The data for the porous forebody (Fig. 6c) show little difference in normal-force coefficient values due to roll and slight changes in side-force coefficient values due to rolling the model. Figure 7 shows the effect of roll angle on the normal-force and side-force characteristics of the 5.0-caliber forebodies at $M_\infty = 0.2$ and angle of attack of 30 deg. The normal force coefficient varied between 2.4–3.2 for the solid forebody model with transition grit, and from 1.4 to 2.2 for the solid forebody model without transition grit. However, the normal force coefficient varied between 2.6–2.7 for the porous forebody model from −90- to 180-deg roll. The side force coefficient is seen to vary from −0.1 to 0.2 for the porous forebody, from −2.4 to 2.8 for the fully gritted surface, and from −2.2 to 2.6 for the free transition condition. Figure 7 shows how effective the passive porous forebody is at reducing the asymmetric loading conditions on axisymmetric forebodies typical of missiles and forebodies of fighter aircraft.

It was also of interest to determine the amount of porous surface area required to eliminate asymmetrical loading conditions. Figure 8 shows the normal-force and side-force coefficient data for the fineness ratio 5.0 tangent-ogive, porous model with various extents of porosity [i.e., fully porous, 1-caliber (4-in.) porous, 2-calibers (8-in.) porous, and 3-calibers (12-in.) porous]. The normal force coefficient values are nearly the same for all four porosity extents with the 1.0-caliber

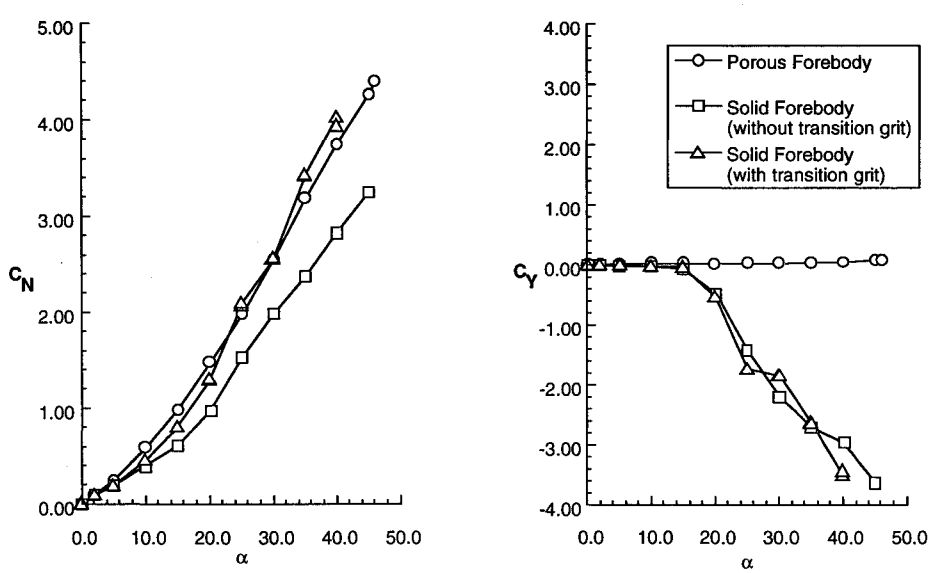

Fig. 5 Effect of transition grit on the normal-force and side-force characteristics of the 5.0-caliber forebodies at $M_\infty = 0.2$.

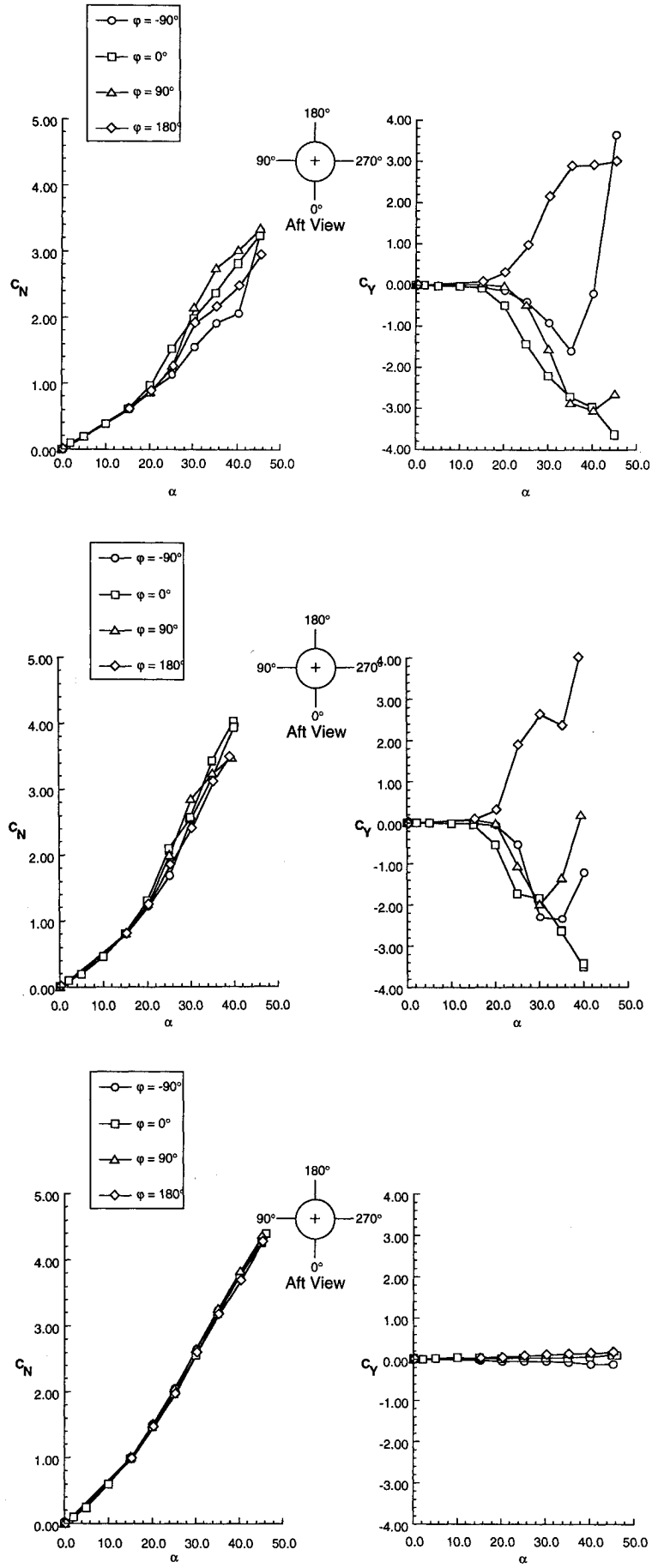

Fig. 6 Effect of roll angle on the normal-force and side-force characteristics of the 5.0-caliber forebodies at M_∞ = 0.2: a) solid body without transition grit, b) solid forebody with transition grit, and c) porous forebody.

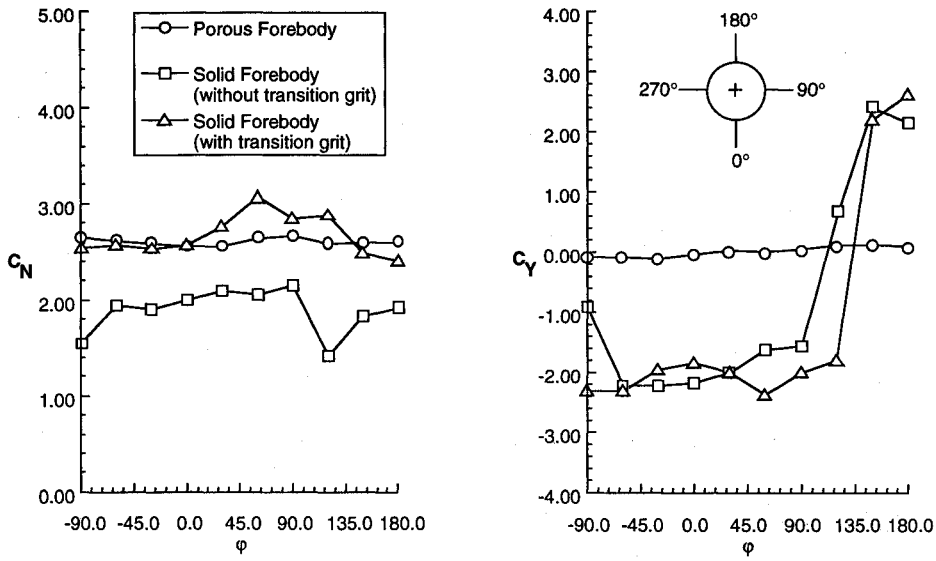

Fig. 7 Effect of roll angle (φ) on the normal-force and side-force characteristics of the 5.0-caliber forebodies at $M_\infty = 0.2$ and $\alpha = 30$ deg.

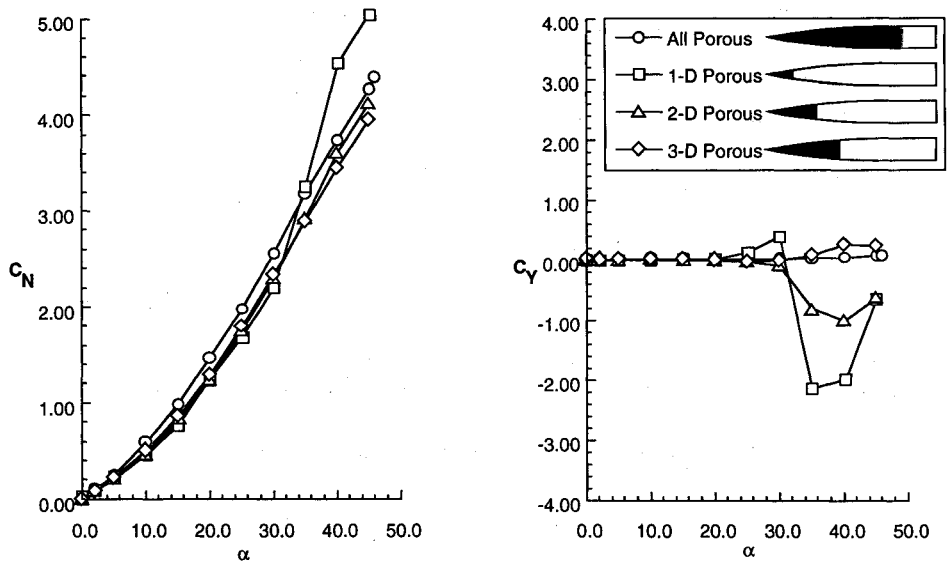

Fig. 8 Effect of porosity extent on the normal-force and side-force characteristics of the 5.0-caliber porous forebody at $M_\infty = 0.2$.

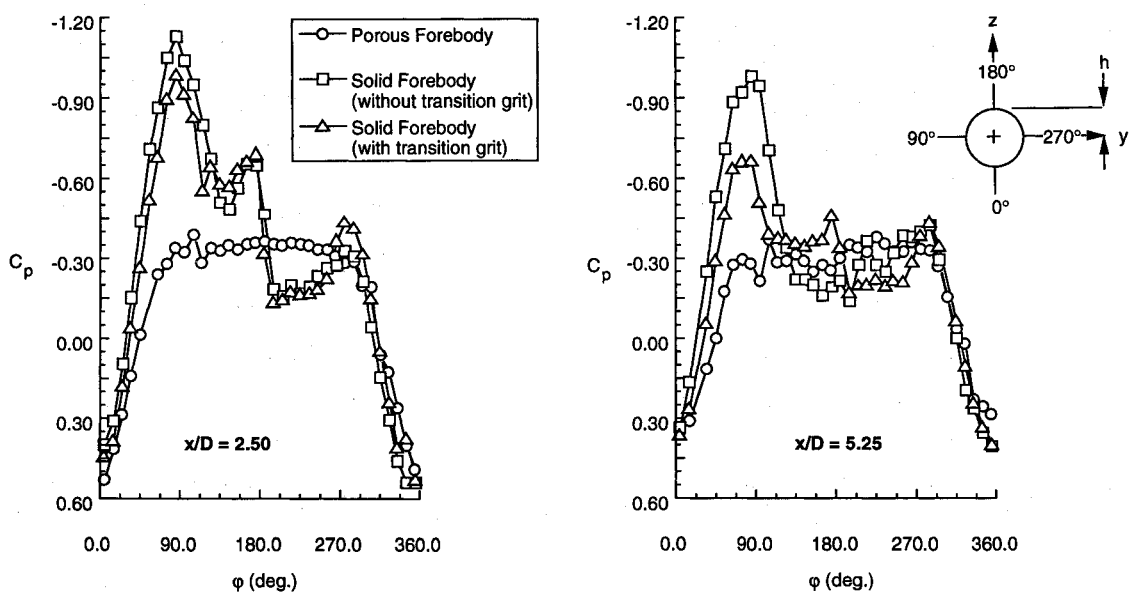

Fig. 9 Comparison of the circumferential pressure distributions of the 5.0-caliber porous forebody at $M_\infty = 0.2$ and $\alpha = 35$ deg.

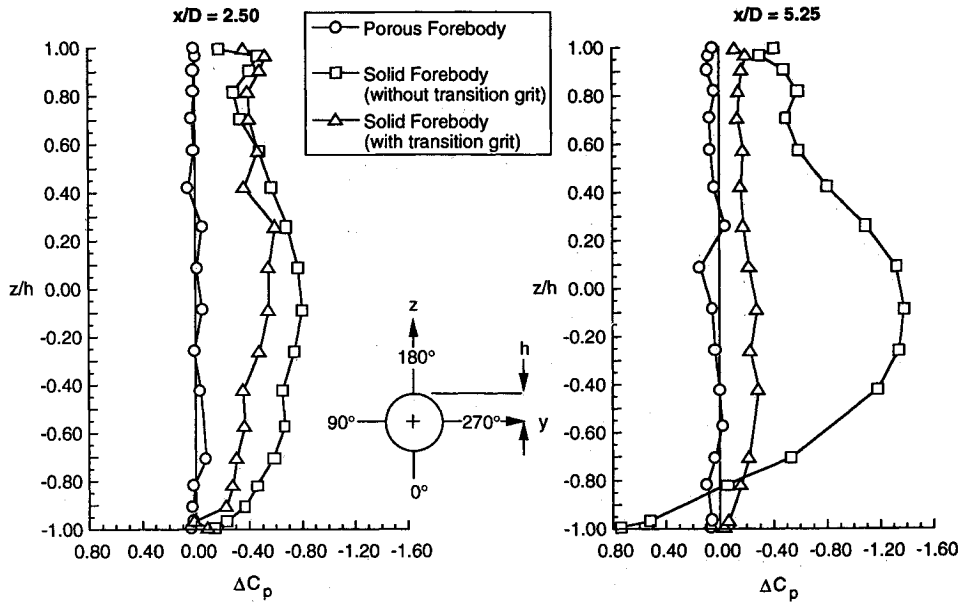

Fig. 10 Graphic representation of the origin of the side force from the asymmetric pressure distributions on the 5.0-caliber tangent-ogive forebodies at $M_\infty = 0.2$ and $\alpha = 35$ deg. $\Delta C_p = (C_p)_{\text{right-hand side}} - (C_p)_{\text{left-hand side}}$.

porous extent providing the highest values above 35-deg angle of attack. The side force coefficients are relatively low for porosity extent of 3 calibers (12 in.) or more, with increasing side force occurring for extent of porosity values less than 3 calibers. However, the C_Y values are still much lower than those found for the fully solid forebodies. These data show that asymmetric loading conditions can be drastically reduced with relatively small amounts of porous surface area.

Forebody Surface Pressure Distributions

Surface pressures were also measured at two locations on each model. In Fig. 9, surface pressure coefficient data is shown for the porous forebody model, the solid forebody model without transition grit, and the solid forebody model with transition grit for the fineness ratio 5.0 tangent-ogive forebody for a Mach number of 0.20 and angle of attack of 35 deg. The data show that the solid surface models have large asymmetric pressure distributions at both stations, causing the large side forces seen in earlier force data plots. The data show that the porous forebody has nearly symmetric pressure loading at both pressure orifice stations with slight asymmetries, possibly due to the porous surface area not extending to the base of the model. Asymmetries originating at the base of the model could start there and move forward. The slight asymmetric side forces seen in Fig. 5 for the porous forebody at 45 deg and the slightly asymmetric pressure distributions at the 5.25-caliber pressure orifice location in Fig. 9 could be due to this effect. Figure 10 represents the data as a delta C_p which is calculated by subtracting the C_p value from the left side of the model from the corresponding C_p value on the right side of the model. These values are plotted against z/h values from -1.0 (bottom of the model) to 1.0 (top of the model). The integrated area of the ΔC_p curve corresponds to a local side force. Both solid surfaced forebodies have quite large values of ΔC_p, and thus a side force (at both body stations) as was seen from the previous force plots. The porous forebody provides essentially no side force at 35 deg.

Concluding Remarks

An experimental investigation of the effect of passive porosity at reducing asymmetric loading conditions has been conducted on two tangent-ogive, forebody shapes in the 7-ft by 10-ft high-speed wind tunnel at Mach numbers of 0.2, 0.5, and 0.8. Force and moment data and surface pressure data were obtained on two solid and two porous forebody models. The normal force coefficient data showed that the porous surface produced turbulent-like boundary-layer conditions, and the side force coefficient data showed the effectiveness of porosity on the forebody. The surface pressure data indicated that the porosity eliminated asymmetries in the pressure loading at the surface of the models. It was also found that small amounts of porous surface area can greatly reduce the asymmetrical conditions.

Data from the pressure tubes located within the plenum indicated that the pressure inside the plenum was nearly constant and that the velocity of the flow inside the plenum was very low.

This preliminary study on the effectiveness of porosity for the elimination of side forces on axisymmetric forebodies up to high angles of attack shows very promising results. Many questions arise in the exact physics of the flow around and through the porous regions of the models, but this initial study gives hope for a simple, low-cost, passive fix to the problem of asymmetric loading conditions on axisymmetric bodies at high angles of attack.

Acknowledgments

M. J. Hemsch was supported in this work by the Transonic Aerodynamics Branch of NASA Langley Research Center under Contract NAS1-19000. The authors wish to thank Richard M. Wood who along with S. X. S. Bauer developed the passive porosity concept for alleviating asymmetric loadings on forebodies and helped design the porous forebody models.

References

[1]Allen, H. J., and Perkins, E. W., "A Study of the Effects of Viscosity on Flow over Slender Inclined Bodies of Revolution," NACA TR 1048, Dec. 1951.

[2]Letko, W., "A Low-Speed Experimental Study of the Directional Characteristics of a Sharp-Nosed Fuselage Through a Large Angle-of-Attack Range at Zero Angle of Sideslip," NACA TN 2911, July 1953.

[3]Coe, P. L., Jr., Chambers, J. R., and Letko, W., "Asymmetric Lateral-Directional Characteristics of Pointed Bodies of Revolution at High Angles of Attack," NASA TN D-7095, Nov. 1972.

[4]Pick, G. S., "Investigation of Side Forces on Ogive-Cylinder Bodies at High Angles of Attack in the $M = 0.5$ to 1.1 Range," AIAA Paper 71-570, June 1971.

[5]Clark, W. H., and Peoples, J. R., "Occurrence and Inhibition of Large Yawing Moments During High Incidence Flight of Slender Missile Configurations," AIAA Paper 72-968, Sept. 1972.

[6]Jorgensen, L. H., and Nelson, E. R., "Experimental Aerodynamic Characteristics for a Cylindrical Body of Revolution with Various Noses at Angles of Attack from 0° to 58° and Mach Numbers from 0.6 to 2.0," NASA TM X-3128, Dec. 1974.

[7]Jorgensen, L. H., and Nelson, E. R., "Experimental Aerodynamic Characteristics for a Cylindrical Body of Revolution with Side Strakes and Various Noses at Angles of Attack from 0° to 58° and Mach Numbers from 0.6 to 2.0," NASA TM X-3130, March 1975.

[8]Jorgensen, L. H., and Nelson, E. R., "Experimental Aerodynamic Characteristics for Bodies of Elliptic Cross Section at Angles of Attack from 0° to 58° and Mach Numbers from 0.6 to 2.0," NASA TM X-3129, Feb. 1975.

[9]Keener, E. R., and Chapman, G. T., "Onset of Aerodynamic Side Forces at Zero Sideslip on Symmetric Forebodies at High Angles of Attack," AIAA Paper 74-770, Aug. 1974.

[10]Keener, E. R., and Taleghani, J., "Wind Tunnel Investigation of the Aerodynamic Characteristics of Five Forebody Models at High Angles of Attack at Mach Numbers from 0.25 to 2.00," NASA TM X-73,076, Dec. 1975.

[11]Keener, E. R., Chapman, G. T., and Kruse, R. L., "Effects of Mach Number and Afterbody Length on Onset of Asymmetric Forces on Bodies at Zero Sideslip and High Angles of Attack," AIAA Paper 76-66, Jan. 1976.

[12]Keener, E. R., Chapman, G. T., Cohen, L., and Taleghani, J., "Side Forces on a Tangent Ogive Forebody with a Fineness Ratio of 3.5 at High Angles of Attack and Mach Numbers from 0.1 to 0.7," NASA TM X-3437, Feb. 1977.

[13]Nagamatsu, H. T., and Orozco, R. D., "Porosity Effect on Supercritical Airfoil Drag Reduction by Shock Wave/Boundary Layer Control," AIAA Paper 84-1682, June 1984.

[14]Thiede, P., Krogmann, P., and Stanewsky, E., "Active and Passive Shock/Boundary Layer Interaction Control on Supercritical Airfoils," AGARD-CP-365, May 1984.

[15]Bahi, L., and Ross, J. M., "Passive Shock Wave/Boundary Layer Control for Transonic Airfoil Drag Reduction," AIAA Paper 83-0137, Jan. 1983.

[16]Nagamatsu, H. T., Brower, W. B., Jr., Bahi, L., and Marble, S. K., "Investigation of Passive Shock Wave/Boundary Layer Control for Transonic Airfoil Drag Reduction," Rensselaer Polytechnic Inst., First Annual Report for NASA Grant NSG 1624, Troy, NY, Oct. 1979–Sept. 1980.

[17]Savu, G., Trifu, O., and Dumitrescu, L. Z., "Suppression of Shocks on Transonic Airfoils," *Proceedings of the International Symposium on Shock Tubes and Waves* (Sydney, Australia), New South Wales Univ. Press, Kensington, New South Wales, Australia, Aug. 1983, pp. 105–113.

[18]Savu, G., and Trifu, O., "Porous Airfoils in Transonic Flow," *AIAA Journal*, Vol. 22, No. 7, 1984, pp. 989–991.

[19]Page, M. A., and Riley, N., "The Free Interaction in a Supersonic Flow over a Porous Wall," *Quarterly Journal of Mechanics and Applied Mathematics*, Vol. 38, Jan. 1985, pp. 79–92.

[20]Marble, S. K., "Transonic Wind Tunnel Blockage Minimization Using a Variable Porosity Plate," M.S. Thesis, Rensselaer Polytechnic Inst., Troy, NY, May 1981.

[21]Clarke, J. F., "Regular Reflection of a Weak Shock Wave from a Rigid Porous Wall," *Quarterly Journal of Mechanics and Applied Mathematics*, Vol. 37, Dec. 1984, pp. 87–111.

[22]Wilcox, F. J., "Experimental Investigation of the Effects of a Porous Floor on Cavity Flow Fields at Supersonic Speeds," NASA TP 3032, Nov. 1990.

[23]Miller, B. A., "A Novel Concept for Subsonic Inlet Boundary-Layer Control," *Journal of Aircraft*, Vol. 14, No. 4, 1977, pp. 403, 404.

[24]Modi, V. J., Cheng, C. W., Mak, A., and Yokomizo, T., "Reduction of the Side Force on Pointed Forebodies Through Add-On Tip Devices," AIAA Paper 90-3005, June 1990.

[25]Henderson, W. P., "Overview of the Applied Aerodynamics Division," NASA TM 102698, June 1991.

[26]Bauer, S. X. S., and Hernandez, G., "Reduction of Cross-Flow Shock-Induced Separation with a Porous Cavity at Supersonic Speeds," AIAA Paper 88-2567, June 1988.

[27]Roach, P. E., and Turner, J. T., "Premature Boundary Layer Transition Caused by Surface Static Pressure Tappings," *Aeronautical Journal*, Vol. 92, No. 912, 1988, pp. 63–68.

[28]Hall, R. M., Erickson, G. E., Banks, D. W., and Fisher, D. F., "Ground Tests and Flight: Advances in High-Alpha Experimental Aerodynamics," Vol. 1, Pt. 1, Paper 4, *NASA High Angle-of-Attack Technology Conference*, NASA Langley Research Center, NASA 3149, Hampton, VA, Oct.–Nov. 1990, pp. 69–115.

[29]Ericsson, L. E., and Reding, J. P., "Asymmetric Vortex Shedding from Bodies of Revolution, Tactical Missile Aerodynamics," edited by M. J. Hemsch and J. N. Nielsen, Vol. 104, Progress in Astronautics and Aeronautics, AIAA, New York, 1986, Chap. VII, pp. 243–296.

[30]Moskovitz, C. A., Hall, R. M., and DeJarnette, F. R., "Combined Effects of Nose Bluntness and Surface Perturbations on Asymmetric Flow Past Slender Bodies," *Journal of Aircraft*, Vol. 27, No. 10, 1990, pp. 909, 910.